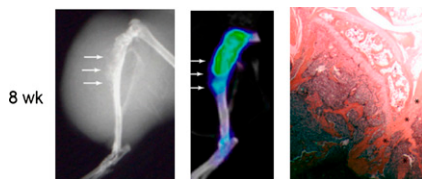


New guidelines introduced: Goldsmith provides perspective on practice guidelines for breast scintigraphy with breast-specific γ -cameras, which appear in this month's issue of *Journal of Nuclear Medicine Technology*. **Page 1823**

Guidelines alert: Tulchinsky offers commentary and details on new and revised practice guidelines for hepatobiliary scintigraphy, which appear in this month's issue of *Journal of Nuclear Medicine Technology*. **Page 1825**

Molecular ^{18}F -NaF PET imaging: Czerin and colleagues review the mechanisms of ^{18}F -NaF deposition in bone and present model-based approaches to quantify bone perfusion and metabolism in preclinical and clinical applications of bone imaging with PET. **Page 1826**



PERCIST or pattern recognition: Hoffman and Hicks critique a recent framework to quantify reduction in PET tracer uptake after treatment, emphasize the continued interpretive significance of pattern recognition, and preview a related article in this issue of *JNM*. **Page 1830**

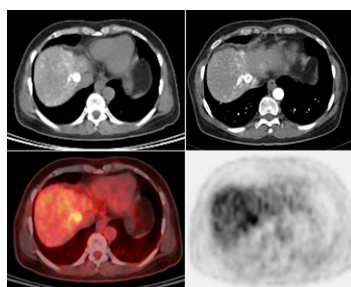
PET/CT after radiofrequency ablation: Singnurkar and colleagues define PET patterns that (in conjunction with clinical parameters) influence local recurrence and may prove useful in identifying patients likely to be cured by ablation or at higher risk for local recurrence. **Page 1833**

Low-dose PET/CT enterography: Shyn and colleagues compare the diagnostic efficacy of low-dose, combined ^{18}F -FDG PET/CT enterography with that of CT

enterography alone in patients with Crohn disease. **Page 1841**

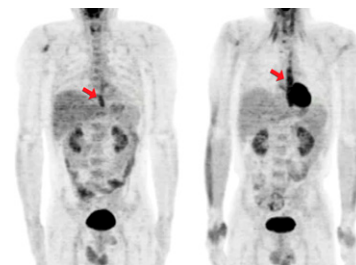


^{18}F -FDG uptake in lipiodolized HCCs: Kim and colleagues evaluate the metabolic characteristics of lipiodolized hepatocellular carcinomas and the diagnostic accuracy of PET/CT in assessing their viability in transcatheter arterial chemoembolized patients. **Page 1849**

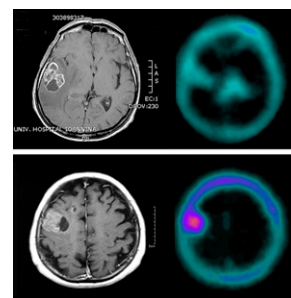


Early PET reference background: Itti and colleagues investigate whether the reference background above which a residual mass is considered positive in the International Harmonization Project criteria should be modified for early ^{18}F -FDG PET evaluation of diffuse large B-cell lymphoma. **Page 1857**

Predicting response in esophageal cancer: Malik and colleagues assess the potential of ^{18}F -FDG PET as an early predictor of histopathologic response to neoadjuvant chemoradiotherapy and overall survival in patients with adenocarcinoma of the esophagus undergoing multimodal therapy. **Page 1863**



Repeatability of metabolic volume test: Frings and colleagues evaluate metabolic volume test-retest variability in ^{18}F -FDG and ^{18}F -FLT PET studies for various commonly used volumes of interest and the relationship to lesion size and relative radiotracer uptake. **Page 1870**



Predicting RIT hematologic toxicity: Baechler and colleagues identify clinical factors for predicting hematologic toxicity in patients with non-Hodgkin lymphoma after radioimmunotherapy with ^{90}Y -ibritumomab tiuxetan or ^{131}I -tositumomab. . . **Page 1878**

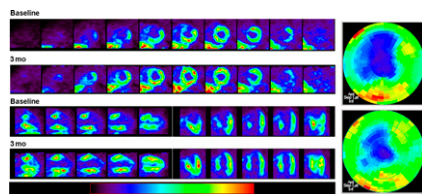
^{123}I -FP-CIT vs ^{123}I -PE2I: Ziebell and colleagues compare the selectivity of these 2 SPECT radioligands for in vivo imaging of dopamine and serotonin transporters in healthy individuals. **Page 1885**

Kinetic modeling of ^{11}C -CUMI-101: Milak and colleagues report on optimal modeling parameters for human PET studies with this serotonin type 1A receptor implicated in the pathophysiol-

ogy of numerous neuropsychiatric disorders. **Page 1892**

PET detection of epileptic foci: Kumar and colleagues evaluate and optimize the lateralization and lobar localization value of epileptic foci of objective voxel-based analysis of ^{18}F -FDG PET scans in a pediatric epilepsy population. . . . **Page 1901**

PET in cardiac stem cell therapy: Castellani and colleagues describe the use of ^{13}N -ammonia and ^{18}F -FDG PET for analysis of cardiac perfusion, metabolism, and function in patients after intracoronary injection of endothelial progenitors or conventional therapy for acute myocardial infarction. **Page 1908**



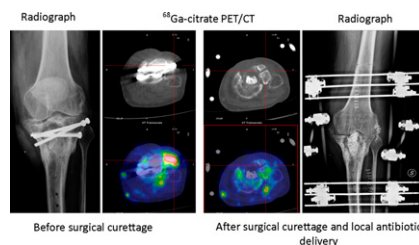
Glucosteroids and effective ^{131}I half-life: Hautzel and colleagues report on the results of a retrospective study to determine the impact of glucocorticoid therapy on effective ^{131}I half-life in radioiodine therapy for Graves disease. . . **Page 1917**

Prediction of survival in glioblastoma multiforme: Alexiou and colleagues investigate the prognostic value of $^{99\text{m}}\text{Tc}$ -tetrafosmin brain SPECT in patients with glioblastoma multiforme. **Page 1923**

Endothelial dysfunction in SLE: Alexánder and colleagues assess the presence

of endothelial dysfunction with ^{13}N -ammonia PET in patients with asymptomatic systemic lupus erythematosus. . . . **Page 1927**

^{68}Ga -citrate in bone infections: Nanni and colleagues study the sensitivity, specificity, positive and negative predictive values, and overall accuracy of ^{68}Ga -citrate PET/CT in a population of patients with suspected bone infections. . . . **Page 1932**



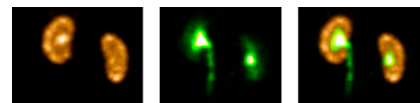
Inflammation imaging: Gotthardt and colleagues provide an educational overview of nuclear medicine imaging in assessment of osteomyelitis, infected vascular prostheses, metastatic infectious disease, rheumatoid arthritis, vasculitis, inflammatory bowel disease, sarcoidosis, and fever of unknown origin. . **Page 1937**

PET/CT in interstitial lung disease: Ambrosini and colleagues evaluate the performance of ^{68}Ga -DOTANOC PET/CT in patients with idiopathic pulmonary fibrosis or nonspecific interstitial pneumonia. **Page 1950**

Angiotensin II receptors after infarction: Higuchi and colleagues use a novel PET radioligand to determine the presence and time course of regional myocardial

upregulation of the angiotensin II type 1 receptor and the blocking efficacy of various anti-RAS agents. **Page 1956**

Micro-SPECT of rat renal function: Melis and colleagues investigate dedicated small-animal SPECT/CT imaging in rats to monitor renal function during follow-up of peptide receptor radionuclide therapy with and without lysine. **Page 1962**



^{90}Y PET dosimetry estimation: Walrand and colleagues report the use of ^{90}Y PET of the first cycle of peptide receptor radionuclide therapy to optimize the injected activity of the following cycles. . . **Page 1969**

^{90}Y imaging for RIT dose assessment: Minarik and colleagues assess the feasibility of quantitative bremsstrahlung imaging to verify predicted absorbed doses in patients undergoing high-dose myeloablative ^{90}Y -ibritumomab treatment. **Page 1974**

Tissue factor imaging of plaque: Temma and colleagues use a $^{99\text{m}}\text{Tc}$ -labeled monoclonal antibody as a molecular probe and evaluate its usefulness in tissue factor-specific imaging in myocardial infarction-prone rabbits. **Page 1979**

ON THE COVER

In a rat model 1 wk after ischemic myocardial damage, PET found focally increased myocardial ^{11}C -KR31173 uptake in a hypoperfused area of reduced ^{13}N -ammonia uptake. After blocking with SK-1080, the increase disappeared. These results provide a rationale for subsequent testing of angiotensin II type 1 receptor-targeted imaging to predict the risk for ventricular remodeling and to monitor the efficacy of drug therapy against the renin-angiotensin system.

See page 1959.

